Surface-Enhanced Raman Scattering Studies on the Interaction of Phosphonate Derivatives of Imidazole, Thiazole, and Pyridine with a Silver Electrode in Aqueous Solution

ARTICLE *in* THE JOURNAL OF PHYSICAL CHEMISTRY B · JULY 2009

Impact Factor: 3.3 · DOI: 10.1021/jp902328j · Source: PubMed

4 AUTHORS, INCLUDING:

Edyta Proniewicz (de domo Podstawka)
AGH Univesrity of Science and Technology …
98 PUBLICATIONS **1,135** CITATIONS
SEE PROFILE

Bogdan Boduszek
Wroclaw University of Technology
111 PUBLICATIONS **1,097** CITATIONS
SEE PROFILE

Surface-Enhanced Raman Scattering Studies on the Interaction of Phosphonate Derivatives of Imidazole, Thiazole, and Pyridine with a Silver Electrode in Aqueous Solution

Edyta Podstawka,*,† Andrzej Kudelski,‡ Tomasz K. Olszewski,§ and Bogdan Boduszek§

Regional Laboratory of Physicochemical Analysis and Structural Research, Faculty of Chemistry, Jagiellonian University, ul. Ingardena 3, 30-060 Krakow, Poland, Faculty of Chemistry, University of Warsaw, ul. L. Pasteura 1, 02-093 Warsaw, Poland, and Organic Chemistry Division, Faculty of Chemistry, Wroclaw University of Technology, ul. Wybrzeże S. Wyspiańskiego 27, 50-370 Wrocław, Poland

Received: March 16, 2009; Revised Manuscript Received: May 28, 2009

Surface-enhanced Raman scattering (SERS) spectra from phosphonate derivatives of N-heterocyclic aromatic compounds immobilized on an electrochemically roughened silver electrode surface are reported and compared to Raman spectra of the corresponding solid species. The tested compounds contain imidazole [**ImMeP** ([hydroxy-(1*H*-imidazol-5-yl)-methyl]-phosphonic acid) and **$(ImMe)_2P$** (bis[hydroxy-(1*H*-imidazol-4-yl)-methyl]-phosphinic acid)]; thiazole [**BAThMeP** ((butylamino-thiazol-2-yl-methyl)-phosphonic acid) and **BzAThMeP** ((benzylamino-thiazol-2-yl-methyl)-phosphonic acid)]; and pyridine (**$(PyMe)_2P$** (bis[(hydroxy-pyridin-3-yl-methyl)]-phosphinic acid) aromatic rings. Changes in wavenumber, broadness, and the enhancement of N-heterocyclic aromatic ring bands upon adsorption are consistent with the adsorption primarily occurring through the N lone pair of electrons with the ring arranged in a largely edge-on manner for **ImMeP** and **BzAThMeP** or in a slightly inclined orientation to the silver electrode surface at an intermediate angle from the surface normal for **$(ImMe)_2P$**, **BAThMeP**, and **$(PyMe)_2P$**. A strong enhancement of a roughly 1500 cm^{-1} SERS signal for **ImMeP** and **$(PyMe)_2P$** is also observed. This phenomenon is attributed to the formation of a localized C═C bond, which is accompanied by a decrease in the ring-surface π-electrons' overlap. In addition, more intense SERS bands due to the benzene ring in **BzAThMeP** are observed than those observed for the thiazole ring, which suggests a preferential adsorption of benzene. Some interaction of a phosphonate unit is also suggested but with moderate strength between biomolecules. The strength of the P═O coordination to the silver electrode is highest for **ImMeP** but lowest for **BzAThMeP**. For all studied biomolecules, the contribution of the structural components to their ability to interact with their receptors was correlated with the SERS patterns.

Introduction

In recent years, organophosphorus compounds have been of great interest and have found a wide range of applications in the area of medicinal, agricultural, and industrial chemistry, based on their interesting biological and physical properties, as well as their utility as synthetic intermediates.[1,2] Among many known phosphorus compounds (phosphane oxides, phosphonic or phosphinic acids, and their esters), α-functionalized phosphonates and α-amino- and α-hydroxyphosphonates, in particular, have received considerable attention due to their biological activity.[3−5] α-Amino- and α-hydroxyphosphonates are structural analogues of natural α-amino- or α-hydroxycarboxylic acids, in which the weakly basic, mononegative, planar, and less bulky carboxylic group is replaced by a considerably more basic, dinegative, tetrahedral phosphonic or related group. These molecules act as excellent enzyme inhibitors[6,7] and are potent antibacterial,[8,9] antiviral,[10,11] and anticancer agents.[12,13] Often, this biological activity is related to the metal binding ability of those molecules.[14] The heterocyclic phosphonates presented here reveal also inhibitory activity toward chymotrypsin from bovine pancreas (12−25% of inhibition).[15] It was also found that the character of the heterocyclic moiety has a marginal influence on the power of inhibition, and therefore the phosphorus-containing part is expected to play the main role in the inhibition process. This is in good agreement with literature data, where phosphorus diphenyl esters are known to be excellent irreversible, slow binding, competitive inhibitors for chymotrypsin-like and trypsin-like serine proteases.[16,17] Moreover, the phosphonate derivatives of thiazole, pyridine, and imidazole presented here were found to be excellent ligands for Cu(II) ions.[18,19] The major factor influencing the high stability of the metal complexes is the involvement of the ligand nitrogen donors of the amino group (in the case of **BAThMeP** and **BzAThMeP**) and of the heterocyclic moiety (in the case of pyridine, imidazole, or thiazole). The hydroxyl groups (in the case of **ImMeP**, **$(ImMe)_2P$**, and **$(PyMe)_2P$**) could also be viewed as potent binding sites at a higher pH. Additionally, in all of these molecules, the phosphonic oxygen may serve as an additional donor, especially at lower pH where protonated species are present.

The biological importance of the aforementioned molecules has motivated us to perform a number of spectroscopic studies on them. Previously, we have applied Fourier-transform Raman spectroscopy, which, among many molecular spectroscopy methods, is a valuable method for the qualitative and quantitative measurement of different structural components for the determination of their nonadsorbed molecular structures.[20] This study

* Corresponding author. E-mail: podstawk@chemia.uj.edu.pl. Phone: +48-12-663-2077. Fax: +48-12-634-0515.
† Jagiellonian University.
‡ University of Warsaw.
§ Wroclaw University of Technology.

10.1021/jp902328j CCC: $40.75
Published on Web 06/25/2009

presented the equilibrium geometries for the ground state and those relevant for biomolecules consisting of 0 to 5 bonded water molecules, as well as complete solid-state vibrational assignments based primarily on density functional theory (DFT) calculations at the B3LYP; 6-31++G** level using Gaussian 03 software. Other than our previous publication, there have been no other reported vibrational studies of these compounds. The present study involves the characterization of adsorbed structures of these species immobilized onto an electrochemically roughened silver electrode surface. The orientation of the surface species and the surface bond is analyzed in detail. We also use the surface-enhanced Raman scattering (SERS) technique to propose a likely mechanism of their adsorption onto this substrate. This technique is a simple and rapid method of probing different types of supramolecular architectures and studying adsorption phenomena at the peptide/protein level.[21−27] On a metal surface/biomolecule interface, the biomolecule has fragments, which directly interact with this surface. These fragments usually determine the adsorption behavior of biomolecules onto given metal surfaces. Therefore, analysis of the SERS signal (enhancement, broadness, and wavenumber) produced from their constituents' functional groups is important for understanding possible ways in which a biomolecule can interact with the surrounding medium, such as how a substrate binds to its receptor. Hence, on the basis of the molecular properties, as well as the capability to form ordered monolayers on metal surfaces, the biomolecules investigated here are expected to be good candidates for the exploration of the relationship between adsorption processes to a silver electrode surface and those to a receptor.

Experimental Section

Peptide Synthesis. The organophosphonic and organophosphinic acids used in this study were synthesized according to a previously described procedure.[18,19] The phosphonic acids used were: **ImMeP** ([hydroxy-(1*H*-imidazol-5-yl)-methyl]-phosphonic acid), **BAThMeP** ((butylamino-thiazol-2-yl-methyl)-phosphonic acid), and **BzAThMeP** ((benzylamino-thiazol-2-yl-methyl)-phosphonic acid). The phosphinic acids used were: **(ImMe)$_2$P** (bis[hydroxy-(1*H*-imidazol-4-yl)-methyl]-phosphinic acid) and **(PyMe)$_2$P** (bis[(hydroxy-pyridin-3-yl-methyl)]-phosphinic acid). The purity and chemical structures of these samples were proved by means of ^{1}H,^{31}P, and ^{13}C NMR spectra (Bruker Avance DRX 300 MHz spectrometer) and electrospray mass spectrometry.

SERS Measurements. To obtain a sufficiently enhanced intensity of the SERS bands, the silver substrates were electrochemically roughened before the adsorption of organic species. Roughening was carried out in a conventional three-electrode cell with a large platinum sheet as the counter-electrode and an Ag/AgCl (1 M KCl) electrode as a reference (all potentials are quoted versus this electrode). The silver was roughened by three successive negative−positive−negative cycles in a 0.1 M KCl aqueous solution from −0.3 to 0.3 V at a sweep rate of 5 mV s^{-1}. The cycling was finished at −0.3 V, and then the silver electrode was maintained at −0.4 V for 5 min. After that, the working electrode was removed at an open circuit potential and carefully rinsed with water.

Raman spectra were recorded with an ISA T64000 (Jobin Yvon) Raman spectrometer equipped with Kaiser SuperNotch-Plus holographic filters, 600 grooves/mm holographic grating, an Olympus BX40 microscope with a 50× long distance objective, and a 1024 × 256 pixel nitrogen-cooled CCD detector. A Laser-Tech model LJ-800 mixed argon/krypton laser provided the excitation radiation at 514.5 nm. The laser power at the sample was set to 1 mW (∼10^4 W/cm^2). The final sample concentration was ∼10^{-4} M.

Results and Discussion

Structurally, **ImMeP** (Figure 1) consists of an imidazole ring with a hydroxymethyl phosphonic acid side chain on the C_4 carbon atom (at position 4). **ImMeP** is neutral in aqueous solutions at physiological pH with a p*K* value of 7.66 for the imidazole nitrogen and a p*K* value of 5.87 for the phosphonate group.[18] Its analogue, **(ImMe)$_2$P**, contains two hydroxy-(1*H*-imidazol-4-yl)-methyl moieties. Just as imidazole does, **ImMeP** and **(ImMe)$_2$P** exist in tautomeric equilibrium with either N_1 or N_3 protonated. The protonated nitrogen is referred to as the pyrrole nitrogen and the unprotonated nitrogen as the pyridine nitrogen. Replacement of 1*H*-imidazole in **(ImMe)$_2$P** by pyridine results in **(PyMe)$_2$P**. The two remaining compounds investigated here, **BAThMeP** and **BzAThMeP**, also consist of an N-heterocyclic aromatic ring, a thiazole ring, substituted at C_2 with *n*-butyl- and benzyl-aminomethyl phosphonic acid, respectively. Both compounds, **BAThMeP** and **BzAThMeP**, exhibit two protonation constants. For **BAThMeP**, the p*K* values equal 8.67 and 4.83 and may be assigned to amino and phosphonate functions, respectively. Similar p*K* values are observed for **BzAThMeP**, namely, 7.56 and 4.71. The protonation constant of the benzylamino-substituted nitrogen in **BzAThMeP** is distinctly lower than that of the *n*-butylamino derivative **BAThMeP**, while the basicities of the phosphonate function are rather similar to each other.[19] Hence, the major species in aqueous solution at physiological pH are the neutral species.

Figure 2 illustrates, for the first time, the SERS spectra of **ImMeP**, **(ImMe)$_2$P**, **BAThMeP**, **BzAThMeP**, and **(PyMe)$_2$P** acids in the spectral range of 1700−550 cm^{-1}. These spectra almost exclusively possess the characteristic Raman bands due to the modes of N-heterocyclic aromatic rings: imidazole (Im), thiazole (Th), and pyridine (Py). Also, the spectral features of the benzyl, phosphonate/phosphinate, or methyl moieties are observed. Table 1 lists the wavenumbers of these bands and their allocation to the normal mode motions. It also summarizes the spectral positions of these bands enhanced in the Raman spectra of these compounds. Further information about normal mode assignments of Im was obtained from the resonance Raman studies on imidazole and imidazolium performed by Hudson, Zgierski, and co-workers, who reported a detailed vibrational analysis of these molecules and their deuterated analogues.[28] The Raman spectroscopic and DFT investigations of **ImMeP**, **(ImMe)$_2$P**, **BAThMeP**, **BzAThMeP**, and **(PyMe)$_2$P** have also provided background for the present experiment.[20] Also, the SERS of Im has been reported by several groups on both silver and copper electrodes[29−32] and on silver sols.[33,34] The SERS of imidazole ring-containing histidine and histamine have also been reported on silver.[35−38] There have been also several reports of the vibrational spectra of thiazole. The vibrational assignment used in this work for **BAThMeP** and **BzAThMeP** is that reported by Palmer et al.[39,40] and El-Azhary.[41] The vibrational assignments reported in ref 20 were used for comparison with the calculated scaled wavenumbers. Relative to imidazole and thiazole, a great amount of macroscopic information concerning the metal−solution interface has been reported for pyridine. Most of the experiments were performed in aqueous solutions. The substrates used include copper, silver, gold electrodes, and silver sols.[42−47]

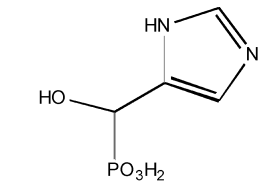

ImMeP
[Hydroxy-(1H-imidazol-5-yl)-methyl]-phosphonic acid

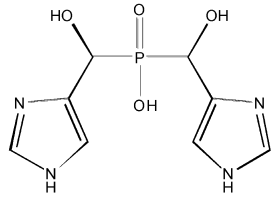

(ImMe)$_2$P
Bis-[hydroxy-(1H-imidazol-4-yl)-methyl]-phosphinic acid

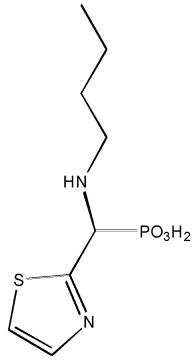

BAThMeP
(Butylamino-thiazol-2-yl-methyl)-phosphonic acid

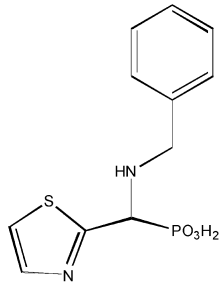

BzAThMeP
(Benzylamino-thiazol-2-yl-methyl)-phosphonic acid

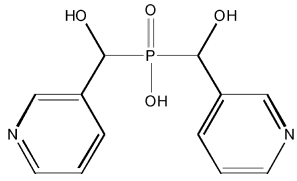

(PyMe)$_2$P
Bis-[(hydroxy-pyridin-3-yl-methyl)]-phosphinic acid

Figure 1. Molecular structures of **ImMeP**, **(ImMe)$_2$P**, **BAThMeP**, **BzAThMeP**, and **(PyMe)$_2$P**.

The SERS spectrum of **ImMeP** exhibits four strong bands in the investigated wavenumber region (Figure 2, top trace). Specifically, these bands are observed at 1501, 1002, 1268, and 1142 cm^{-1}. The former two bands are assigned to in-plane imidazole stretching coupled with C_2-H in-plane bending and in-plane C−H ring deformation vibrations, respectively. The latter two are both due to P═O stretching modes. However, considering the high value of the full width at half-maximum (fwhm) for the 1142 cm^{-1} SERS band (fwhm = 23 cm^{-1}) in contrast to that of the Raman spectrum, we believe that ν_{ip}(Im) may overlap with the 1142 cm^{-1} band (Table 1). It is also noteworthy that a substantial upshift in wavenumber ($\Delta_\nu = 7$ cm^{-1}) of 1501 cm^{-1} and down-shift in wavenumber ($\Delta_\nu = -5$ cm^{-1}) of 1268 cm^{-1} spectral features and also band broadening ($\Delta_{fwhm} = 9$ and 6 cm^{-1}, respectively) between the Raman and SERS (Figure 1) spectra of this molecule are observed. These phenomena suggest that **ImMeP** adsorbs via the pyridine N and =O lone pair of electrons at the silver electrode surface. Also, on the basis of the SERS selection rules,[48−50] enhancement of the in-plane vibrational modes and the hardly detectable enhancement of the out-of-plane modes of adsorbed **ImMeP** indicate that the Im ring is oriented in an end-on or edge-on manner, perpendicular to the surface. This is in agreement with results obtained by Cao et al., who showed that in the potential region from −0.1 to −0.5 V, if Im is oriented perpendicularly with respect to the metal surface, the ring is adsorbed with the edge-on adsorption through the pyridine N atom.[51] These surface selection rules were applied again to ascertain the changes in orientation of the imidazole. We have done our analysis on the basis of the "standard surface selection rules" that were developed from the electromagnetic theory of SERS intensity, which indicates that normal modes of the adsorbed molecule involving changes in molecular polarizability with a component normal to the surface are the most enhanced (since the light at the metal surface is preferentially polarized, the normal component of the electric field is much larger than the tangential component). Recently, more precise so-called Herzberg−Teller SERS surface selection rules have been developed, which can

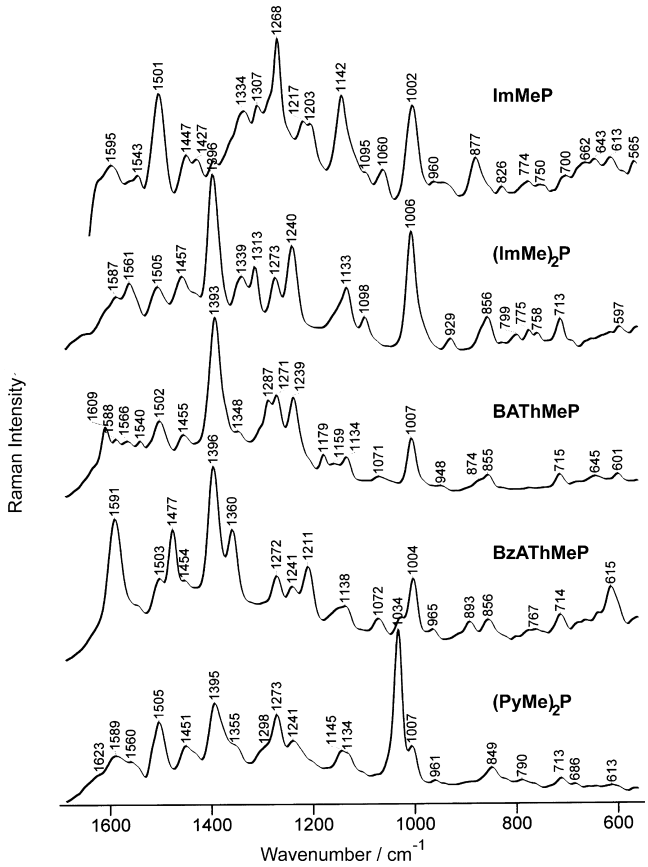

Figure 2. SERS spectra of **ImMeP**, **(ImMe)$_2$P**, **BAThMeP**, **BzAThMeP**, and **(PyMe)$_2$P** immobilized at an electrochemically roughened silver electrode surface in the spectral range of 1700−550 cm^{-1}.

explain on the basis of the analysis of charge-transfer or molecular resonance effects additional enhancement of the nontotally symmetric bands relative to the totally symmetric bands.[52] To apply the Herzberg−Teller SERS surface selection rules, detailed symmetry analysis involving also excited states of adsorbed molecules is required. However, in this contribution, we study molecules with relatively low symmetry (especially after adsorption), and the detailed symmetry analysis is very problematic. Therefore, our orientation analysis is based only on "standard" SERS surface selection rules.

For N-containing heterocycles on a metal surface, two adsorption modes were predicted:[48] edge-on (through the nitrogen atom lone pair of electrons) and flat-on (through the π-electron system of the ring). In brief, for the edge-on orientation, vibrational modes that are out-of-plane are either not present or weakly enhanced compared to the in-plane modes of the adsorbate. The ring breathing vibrations of the adsorbate usually increase in relative intensity upon adsorption, and the wavenumbers for most bands decrease. For the flat-on adsorption, which is relatively weak, the wavenumbers of the modes associated with the ring decrease upon adsorption at more positive potentials, whereas the breathing modes generally upshift in wavenumber as the potential becomes more negative.

Although theoretical calculations and experimental studies showed that four Im ring breathing vibrations should be observed in the Raman spectrum of **ImMeP**, at 1311, 1253, 804, and ca. 700 cm^{-1}, only one band is well-resolved at 1307 cm^{-1} in the SERS spectrum of this biomolecule.[20,36] The observed 4 cm^{-1} down-shift in wavenumber for this band supports immobilization of **ImMeP** through the pyridine N lone pair of electrons. This agrees with studies by Bukowska and co-workers[53] and Sabrana et al.[54] who showed that, at potentials between 0.0 and −0.25 V, the wavenumbers of the Im ring breathing modes usually increase after immobilization of the molecule on the silver electrode, while these wavenumbers decrease at more negative potentials. The relationship between the N lone pair binding versus π-electron system binding has also been described. In general, the shifts in the wavenumbers of Im adsorbed via π-electrons are opposite to those observed for Im adsorbed through the N lone pair of electrons.

Assignment of the medium enhanced spectral features at 1595, 1543, 1447, 1217, 1203, and 1060 cm^{-1} is also straightforward. According to the literature and our previous DFT calculations, they mainly correspond to the Im in-plane vibrations (see Table 1). However, the 1543 and 1447 cm^{-1} bands may also contain a component of the N−H deformation. Cao and co-workers showed that if Im adsorbs through the pyrrole N lone pair of electrons the N−H bond would be nearly horizontal on the surface, and no SERS signal of the in-plane N−H modes should be observed.[51] Hence, the interaction of the pyrrole N lone pair of electrons with the silver electrode surface cannot be ruled out.

Another interesting phenomenon is the position of the 1595 cm^{-1} band (ring ν(C$_4$═C$_5$)), which implies that the imidazole ring of **ImMeP** exists as a 1H rather than a 3H tautomer.[35] Thus, the N$_3$ is the pyridine nitrogen, while N$_1$ corresponds to the pyrrole nitrogen (N$_1$−H).

As mentioned earlier, the two ν(P═O) modes are predominantly enhanced in the SERS spectrum of **ImMeP** immobilized onto the electrochemically roughened silver electrode, indicating a strong P═O···Ag interaction. The position of the higher-wavenumber ν(P═O) is slightly down-shifted in comparison to that observed in the **ImMeP** Raman spectrum. This is due to the slightly decreased double-bond character of the P═O bond when there is coordination with the electrode surface through the ═O atom. Three other spectral features that we attributed to the adsorbed phosphonate moiety are the partially resolved bands at 1427, 1060, and 877 cm^{-1}. The first band is due to the deformation of the PC(H)C fragment, whereas the second one refers to the δ(PCC) mode. The last band is related to the adsorbed C−P−O unit. The medium enhancement of these SERS signals implies that the P═O bond has adopted a tilted orientation with respect to the silver electrode surface. This arrangement would allow the lone electron pairs of both oxygen atoms (═O and −OH) to interact with the silver surface.

Significant spectral changes exist between the **ImMeP** and **(ImMe)$_2$P** deposited onto the electrochemically roughened silver electrode surface. The well-defined and strong 1505, 1273, and 1133 cm^{-1} bands considerably decrease in the **(ImMe)$_2$P** SERS spectrum (Figure 2, second top trace), pointing to a weaker interaction between the N and ═O lone pairs of electrons with the silver electrode surface. Hence, the imidazole ring may change orientation from nearly vertical to become slightly inclined to the silver surface at an intermediate angle from the surface normal. Different from **ImMeP**, the 1273 cm^{-1} band does not shift in wavenumber for **(ImMe)$_2$P** and is only negligibly broadened (Δ_{fwhm} = 3 cm^{-1}) in comparison to its position and width in the **(ImMe)$_2$P** Raman spectrum. Considering this, as well as the fact that its relative intensity is almost one-third that of the **(ImMe)$_2$P** Raman spectrum, we assume that the P═O fragment may be slightly removed from this surface. Other direct evidence for this orientation comes from both the disappearance of the 1427 cm^{-1} band (see Table 1 for the band assignment) and the change in the ratio of the integrated intensity of the 877 cm^{-1} band to that of the 856 cm^{-1} band

Published on June 25, 2009 on http://pubs.acs.org | doi: 10.1021/jp902328j

TABLE 1: Wavenumbers and Proposed Band Assignments for the Raman and SERS Spectra of ImMeP, $(ImMe)_2P$, BAThMeP, BzAThMeP, and $(PyMe)_2P$ Immobilized at an Electrochemically Roughened Silver Electrode Surface[a]

wavenumbers [cm^{-1}]					wavenumbers [cm^{-1}]					wavenumbers [cm^{-1}]			
ImMeP		**$(ImMe)_2P$**		literature assignment for Im[b]	**BAThMeP**		**BzAThMeP**		literature assignment for Th and Bz[c]	**$(PyMe)_2P$**		literature assignment for Py[d]	assignment B3LYP/6-311*[e]
RS	SERS	RS	SERS		RS	SERS	RS	SERS		RS	SERS		
											1623	$\nu_1+\nu_{6b}$	$\nu(C-C)_{Py}+\nu(C-N)_{Py}+\nu(C-H)_{Py}$
1610	1595	1620	1587	$\nu_{ip}(C_4{=}C_5)_{Im}$ (taut N_1)		1609 1588	1605	1591	Bz (ν_{8a}, A_1)		1589	ν_{8a} [ν(Py)], A_1	
	1543		1561	$\nu_{ip}(C_2N_1+C_5N_1)_{Im}+\rho_{inb}(N-H)$	1552	1566 1540	1588		Bz (ν_{8b}, B_2)	1558	1555	ν_{8b}[ν(Py)], B_2	
1494	1501	1493	1505	$\nu_{ip}(C_2N_3+C_4N_3+C_5N_1)_{Im}+\rho_{inb}(C_2-H)$		1502		1503	Bz (ν_{19a}, A_1)		1505	semicircle ν_{19a} [$\delta(CH)_{Py}$], A_1 or $2\nu_4$, A_1	$\rho_t(C-H)_\phi+\nu(C-C)_\phi+\nu(C-N)_\phi$, $\rho_r(N-H)+\rho_s(CH_2)$
							1463	1477	Th (ν_4, A′), Bz (ν_{19b}, B_2)				$\rho_t(C-H)_{Bz}+\nu(C-C)_{Bz}$
1449	1447	1463	1457	ν_{ip}(Im)+$\delta(N_1H)$	1438	1455	1436	1454			1451	ν_{19b} [$\delta(CH)_{Py}$], B_2	$\rho_r(C-H)_\phi+\nu(C-C)_\phi+\nu(C-N)_\phi$
	1427				1423		1420						δ(PC(H)C)), ρ_b(C−OH)
	1396		1396	$\nu(N_1C_2C_3)$ and/or ρ_w(CH)		1393	1385	1396	Th (ν_5 [ν(C═N)], A′)		1395		δ/ρ_b(PC(O)C) ρ_b(PC(N)C)+ δ(PCC)
						1348	1330	1360	Th (ν_6 [ρ_r(CH)+ν(C═N)], A′), Bz (ν_3, B_2)		1355	ν_{14} [$\delta(CH)_{Py}$], B_2	$\rho_r(C-H)_\phi$ +$\nu(C-N)_\phi$+ρ_r(C−H), ρ_b(C−OH), $\rho_w(CH_2)$, $\nu(C-C)_{Bz}$
	1334		1339	ρ_b(CH)									$\nu(C-N)_{Im}+\nu(C-C)_{Im}+\rho_r(C-H)$
1311	1307	1317	1313	$\nu_{ip}(Im)_{breathing}$	1314	1287	1296		Bz (ν_4, B_2)		1298	$2\nu_{6b}$, A_1	$\delta(CH_2/CH3)$, $\rho_r(C-H)+\rho_b(C-OH)+\nu(C-N)_\phi+\rho_t(C-H)_\phi$, $\rho_t(CH_2)+\rho_w(CH_2)+\rho_r(C-H)_{Th}+\rho_r(C-H)$
1273	1268	1273	1273	δ(Im), $\rho_{inb}(C_2H)$		1271	1276	1272		1281	1273		ν(P═O)
1253		1246	1240	$\nu_{ip}(Im)_{breathing}$		1239		1241	Th (ν_7 [ρ_w(CH)], A′)	1242	1241	ν_3 [$\delta(CH)_{Py}$], B_2	$\rho_r(C-H)_{Th}+\nu(C-C)_{Th}$ and/or ρ_r(C−H), $\rho_t(CH_2)$, $\rho_r(CH_2)$, $\delta(CH_3)$ ρ_b(CNH)
1204	1217 1203	1196		δ(Im)	1204		1215	1211	Bz (ν_{7a}, A_1)	1207		ν_{9a} [ν(Py)], A_1	$\nu(P-O)+\rho_b(P-OH)+\rho_r(C-H)$, $\rho_r(C-H)_{Im}$
1176		1169		δ(Im), $\rho_{ipb}(N_1H)$	1172	1179	1188		Bz ($\nu_{9a/15}$, A_1/ B_1)				$\delta(CH_2/CH3)$
	1142		1148[f]			1159	1158	1151[g]			1145		ν(P═O)
1131	1120[f]		1133	ν_{ip}(Im)	1117	1134	1119	1138	Th (ν_8 [ρ_r(CH)], A′)	1119	1134	ν_{15}, B_2	$\nu(C-N)_\phi+\rho_r(C-H)_\phi+\rho_r(C-N)_\phi$, $\nu(C-S)_{Th}$
1093	1095	1097	1098	$\rho_{ipb}(C_5H)$									$\nu(C-N)_{Im}+\rho_r(C-H)_{Im}$
1063	1060	1072		$\rho_{ipb}(CH)_{Im}$	1063	1071	1060	1072	Bz (ν_{18b}, B_2)	1065		ν_{18a} [$\delta(CH)_{Py}$], A_1	δ(PCC) $\nu(C-C)_\phi+\delta(\phi)$, $\nu(C-S)_{Th}$, ν(C−N), ρ_b(CNC),
	1002	1019	1006	$\rho_{in}(CH)_{Im}$	1024	1007	1004	1004	Th (ν_9 [ρ_r(CH)], A′) Bz (ν_{12}, A_1)	1022	1034	ν_{12} [$\nu(Py)_{trig.brething}$], A_1	
								1032	Bz (ν_{18a}, A_1)	1042			
971	960	984		ν(CC)$_{Im}$, $\rho_{oopb}(C_2H)_{Im}$	985						1007	ν_1 [$\nu(Py)_{totally\ sym..brething}$], A_1	
904	935	922	929	γ_{oop}(NH), δ(Im)	914	948	958	965	Bz ($\nu_{5/17a}$, B_1/ A_2)				ρ_b(P−OH), ν(P−O)+ν(C−P)
	877		868	ρ_{ipb}(Im),$\nu(CC)_{Im}$	877	874	875	893	Th ($\nu_{10/11}$ [δ(Th)], A')				ν(P−O)+ν(C−P), $_b$(P−OH), ν(C−C)
842			856	$\rho_{oopb}(CH)_{Im}$		855	844	856	Th (ν_{14}, A″), Bz (ν_{10a}, A_2)	845	849		$\rho_w(C-H)+\nu(P-O)+\rho_b(P-OH)+\nu(C-P)$
804	826	821	799	$\nu(Im)_{breathing}$	790		802		Th (ν_{15}, A″,ρ_w(CH))	825	790		$\rho_w(C-H)_\phi+\delta_{oop}(\phi),\nu_{as}$(OPO)
	774	771	775	$\rho_{oopb}(CH)_{Im}$	767			767	Th (ν_{12}, A′)				$\rho_t(CH_2)_{Th}$, $\delta_{oop}(Bz)+\rho_w(C-H)+\rho_w(C-H)_{Bz}$ ν(C−P)+ρ_s(CCP), ν_s(OPO)
742	750		758	$\gamma_{oop}(CH)_{Im}$									$\rho_w(C-H)_{Im}+\delta_{oop}(Im)+\rho_b(CCP)+\nu(P-O)+\nu(C-C)$
	700		713	$\nu(Im)_{breathing}$	727	715	740	714	Th (ν_{16} [ρ_w(CH)], A″) Bz (ν_1, A_1)	733	713	ν_4 [ρ_t(Py)], B_1	$\nu(C-S)_{Th}+\rho_w(N-H)+\nu(C-C)_{Th}$, $\delta_{oop}(Bz)+\rho_w(C-H)_{Bz}$, ν(C−P)+ρ_b(PCO), $\delta_{oop}(\phi)+\rho_w(C-H)_\phi$
668	662			γ_{oopb}(Im)							686	ν_{11} [$\rho_t(CH)_{Py}$], B_1	ν(C−P)+$\delta_{oop}(\phi)+\rho_b$(PCO)+$\nu$(P−O), ρ_{tors}(P−OH)
636	643	644			637	645	638		ρ_w(CPO), $\delta_{as}(PO_2H)$	644		ν_{6b} [δ(Py)], B_2	$\delta_{oop}(\phi)+\rho_b$(CCP)+$\rho_b$(CCO)
	613		597	ρ_{oopb}(Im)	595	601	618	615	Th (ν_{17}, A″) Bz (ν_{6b}, B_2)	621	613	ν_{6a} [δ(Py)], A_1	

[a] Abbreviations: Im, imidazole; Th, thiazole; Bz, benzyl; and Py, pyridine rings; ϕ, aromatic ring; ν, stretching; δ, deformation; ρ_w, wagging; ρ_b, bending; ρ_t, twisting; ρ_r, rocking; ρ_s, scissoring, A″ or $_{oop}$, out of plane; and A′ or $_{ip}$, out of plane vibrations; γ, torsion. [b] Assignment made on the basis of refs 22−32. [c] Assignment made on the basis of refs 33−35. [d] Assignment made on the basis of refs 36−41. [e] Assignment made on the basis of refs 11 and 17. [f] Based on the deconvolution procedure of the complex bands. [g] *s* = shoulder.

from roughly 4 for **ImMeP** to 0.8 for **(ImMe)$_2$P**. As a consequence, the former band exists as a shoulder of the latter one, and two new bands emerge. First, a broad (FWFM = 23 cm^{-1}) enormously enhanced spectral feature characteristic of $N_1C_2C_3$ stretching/C−H ring wagging and PC(O)C deformation vibrations appears at 1396 cm^{-1} and indicates that the **(ImMe)$_2$P** adsorbs via these fragments. Second, a band located at 1240 cm^{-1} appears due to the imidazole ring breathing vibrations that does not correlate with any band of the **ImMeP** SERS spectrum. The broadening and down-shift in wavenumber of this band are slight and within 3 and −6 cm^{-1}, respectively. Also, little change of the relative band intensity is observed in comparison with that of the Raman spectrum. Our data show that another ring breathing mode (1317 cm^{-1}, Raman → 1313 cm^{-1}, SERS) also down-shifts in wavenumber by −4 cm^{-1}. In addition, the SERS relative intensity increases 4-fold in comparison to that exhibited in the Raman spectrum. At the same time, an increase of the relative intensities of the 1133, 1098, and 1006 cm^{-1} bands is also observed, supporting slight rotation of the Im on the silver electrode surface. It can also be found that the out-of-plane modes mainly below 950 cm^{-1} (929 cm^{-1} (γ_{oop}(NH), δ(Im)); 856 cm^{-1} ($\rho_{oop}(CH)_{Im}$); 775 cm^{-1} ($\rho_{oopb}(CH)_{Im}$); and 758 cm^{-1} ($\gamma_{oop}(CH)_{Im}$)) are further enhanced. This may indicate some preference for an imidazole orientation on the silver surface for which both the in-plane and out-of-plane modes are present. On the basis of these and surface selection rules, we believe that the differences between the SERS spectra of **ImMeP** and **(ImMe)$_2$P** immobilized onto the silver electrode surface are due to the deviation from the edge-on orientation of the imidazole ring for **ImMeP** to a slightly inclined orientation to the silver surface at an intermediate angle from the surface normal for **(ImMe)$_2$P**. This change is accompanied by an alternation in the orientation of the phosphonate moiety, which no longer strongly interacts with the silver electrode surface but is instead oriented in a manner allowing interaction between the PC(O)C fragment and this surface.

The most intense spectral feature of the SERS spectra of **BAThMeP** and **BzAThMeP** immobilized onto the silver electrode surface is the clearly resolved broad (fwhm = ∼25 cm^{-1}) band observed at roughly 1393 cm^{-1}. This band does not correspond to any band in the **BAThMeP** Raman spectrum, while for **BzAThMeP** it corresponds to the 1385 cm^{-1} Raman band. According to Palmer,[40] this is mainly due to the C═N stretching vibration of the thiazole ring (ν_5). However, at this wavenumber range, our DFT calculations predict the presence of bending CN(H)C vibrations coupled with PCC motions (see Table 1).[20] Hence, we may imply that both thiazo molecules adsorb on the silver surface through the C═N and/or CN(H)C fragments. Other similarities between these SERS spectra denote the appearance of the 1502, 1271, 1239, 1159, 1134, 1071, 855, and 715 cm^{-1} bands (see Table 1 for the band assignment). The wavenumbers of these bands in both spectra are similar and within 4 cm^{-1}. Also, their relative intensities are comparable, except for those of the 1271 and 1239 cm^{-1} SERS signals. In the case of **BzAThMeP**, the signals are less enhanced than those of **BAThMeP**. This may be suggestive of the weaker interaction of the P═O and C−H Th ring moieties with the silver electrode surface in the case of **BzAThMeP**. An interesting spectral feature is found at 1007 and 1004 cm^{-1} in the SERS spectra of **BAThMeP** and **BzAThMeP**, respectively, with a symmetric shape for both biomolecules. Although for **BzAThMeP** the relative SERS intensity is slightly above one-fourth of that in its Raman spectrum, for **BAThMeP**, it is only decreased by 50%. In addition, a shoulder (1032 cm^{-1}) due to the ν_{18a} mode of the benzene ring vibrations emerges in the **BzAThMeP** SERS spectrum at the higher wavenumber side of this band. Five additional bands also emerge in this spectrum at 1591, 1477, 1360, 1211, and 615 cm^{-1}. All of these bands exhibit pronounced enhancement and are assigned to the benzene ring modes (see Table 1). However, the asymmetric shape and the high value of fwhm = 28 cm^{-1} for the 615 cm^{-1} band in comparison to those parameters in the **BAThMeP** SERS spectrum may suggest that the Th mode overlaps with the benzene mode. Therefore, we conclude that for this biomolecule the benzene ring preferentially interacts with the silver electrode surface and suggest that the 1004 cm^{-1} band of **BzAThMeP** corresponds to the benzene ring breathing mode (ν_{12}), whereas the 1007 cm^{-1} SERS signal of **BAThMeP** is due to the thiazole C−H rocking vibrations (ν_9). For **BzAThMeP**, neither a down-shift in wavenumber (Δ = 0 cm^{-1}) nor significant band broadening (Δ_{fwhm} = 3 cm^{-1}) is observed for this mode in comparison to its position in the Raman spectrum. Together with the alternation of its enhancement, this implies that the direct benzene π-electron interaction with the electrochemically roughened silver substrate should be rather low. This is probably due to the longer distance of the benzene ring from this surface. On the other hand, for **BAThMeP**, both the 11 cm^{-1} down-shift in wavenumber and the 6 cm^{-1} broadening of this band with respect to its position and width in the Raman spectrum indicate that the strength of the interaction between the thiazole C−H ring fragments and the silver electrode is moderated.

Another surprising phenomenon is the observation of the enormous enhancement of the ν_{8a} mode of the benzene ring in the SERS spectrum of **BzAThMeP** deposited onto the silver electrode surface. This observation together with the lack of changes in the ν_{12} mode wavenumber and width (see discussion above) may suggest that the benzene ring is adsorbed in the electrochemical environment. This conclusion is in agreement with the results by Otero and co-workers who showed that there is no metal−aromatic ring interaction unless there is a significant down-shift in the wavenumber of the ring mode bands, especially ν_1 and ν_{12}.[55,56]

These results show that the **BzAThMeP** thiazole ring interacts mainly via the C═N unit (close to edge-on mode) and/or CN(H)C fragment and the benzene ring (not directly due to the distance effects) with the silver electrode surface. On the other hand, the phosphonate moiety of this biomolecule only assists in this interaction, as in the case of **BAThMeP**. However, the strength of this interaction is slightly higher for **BAThMeP** than for **BzThMeP**. The C═N and C−H fragment of the Th ring, which is slightly inclined to the silver surface at an intermediate angle from the surface normal and/or CN(H)C fragment, is also involved in the **BAThMeP** adsorption process. Medium-low enhanced vibrational bands originating from the $-CH_3$ group are also clearly visible in the SERS spectrum of **BAThMeP** at 1287 and 1179 cm^{-1}. We interpreted these bands as resulting from the assistance of the terminal group of the aliphatic side chain in the adsorption process of this biomolecule.

Not all the SERS signals of **(PyMe)$_2$P** deposited onto the silver electrode surface (Figure 2, bottom trace) closely agree with its Raman spectral features. However, there is reasonable agreement between the Raman profile of **(PyMe)$_2$P** and the results obtained for pyridine nonbonded and bonded on the silver electrode surface.[20,47] Important differences between the SERS and Raman spectra of **(PyMe)$_2$P** are the disappearance of the formerly detected Raman bands at 1207 (Py (ν_{9a}), A_1 class of symmetry) and 1065 cm^{-1} (Py (ν_{18a}), A_1), a prominent decrease in the relative intensity of the 1623 ($\nu_1+\nu_{6b}$), 1007 (ν_1), and

733 cm^{-1} (ν_4) bands and an increase in the enhancement of the 1505 (ν_{19a} or $2\nu_4$), 1395 (δ(PC(O)C), 1273 (ν(P═O), 1145 (ν(P═O), 1134 (ν_{15}), and 1034 cm^{-1} (ν_{12}) spectral features (please note that the assignments of the bands and the symmetry symbols are adopted according to the assignments of the bands in the spectrum of unsubstituted pyridine, and therefore those symbols should be considered only as an assistance in the analysis of the spectra). As can be seen, most of these bands are ascribed to the Py ring vibrations. Hence, we conclude that **(PyMe)$_2$P** interacts with the silver electrode mainly through Py. To choose the correct manner of this interaction, the changes in the enhancement, position and width of these bands should be analyzed. For example, 1034 and 1007 cm^{-1} bands due to the Py trigonal and the Py totally symmetric mode, respectively, shift to the lower wavenumbers by -8 and -15 cm^{-1} upon adsorption. Also, upon adsorption, their bandwidth changes ($\Delta_{fwhm} = \sim 6$ cm^{-1}). This is a trend observed not only for these two modes but in general for all enhanced bands in the SERS spectrum of **(PyMe)$_2$P**. The totally symmetric in-plane modes of the **(PyMe)$_2$P** Raman spectrum, ν_{9a} and ν_1, become relatively weak for **(PyMe)$_2$P** adsorbed on the silver electrode surface. Instead, the semicircle ν_{19a} mode emerges. The second mode from the doubly degenerated semicircle stretches, the ν_{19b} mode ($\sim$1451 cm^{-1}), is also enhanced. The presence of ν_{19b} can be explained by invoking the possibility of forming localized C═C bonds in the Py ring when binding to the silver electrode surface. Therefore, the pyridine ring-surface π overlap becomes weaker. In light of the above results, we rule out that the pyridine ring adopts a slightly inclined orientation to the silver surface at an intermediate angle from the surface normal. In addition, the P(═O)C(O)C fragment of this molecule assists in this binding. Some information about the rearrangement of this fragment on the silver surface can be inferred by the behavior of three bands mentioned earlier, at 1395, 1273, and 1145 cm^{-1}. The observed abrupt growth in the relative intensity of these spectral features, in comparison to those in the Raman spectrum, implies that the lone pairs of electrons of both oxygen atoms (═O and C−O) are involved in the interaction with the silver electrode surface. This is possible if both P═O and C−O moieties are oriented approximately in the same direction.

Conclusions

This paper reports the results of the surface-enhanced Raman spectroscopy (SERS) of phosphonate derivatives of N-heterocyclic aromatic compounds, such as **ImMeP**, **(ImMe)$_2$P**, **BAThMeP**, **BzAThMeP**, and **(PyMe)$_2$P**, immobilized onto an electrochemically roughened silver surface. The power of SERS as a technique for generating spectral fingerprints of analytes that are highly similar in structure using easily prepared substrates and relatively simple instrumentation is illustrated. By analyzing the position, broadness, and relative intensity of the enhanced bands due to vibrations of specific molecular fragments, a mechanism of adsorption on this surface is proposed for the above-mentioned biomolecules and is relevant to the mechanism of substrate−receptor interaction.

The SERS spectra of **ImMeP**, **(ImMe)$_2$P**, **BAThMeP**, **BzAThMeP**, and **(PyMe)$_2$P** deposited onto the silver electrode surface show bands due to vibrations of moieties that were in close contact with the surface. These include the imidazole, thiazole, pyridine, and benzene rings and also the phosphonate group. Because most of the enhancements in the SERS spectra were observed for the vibrations of these moieties, it seems reasonable to conclude that the N lone pair of electrons of the N-heterocyclic aromatic rings of these biomolecules interacts with the silver electrode. In the case of **ImMeP** and **BzAThMeP**, this interaction occurs for the rings oriented in a largely edge-on manner, whereas for **(ImMe)$_2$P**, **BAThMeP**, and **(PyMe)$_2$P**, it occurs for the rings slightly inclined to the silver electrode surface. In addition, upon surface binding, formation of the localized C═C ring bond is observed for **ImMeP** and **(PyMe)$_2$P**, while the competitive interaction of the benzene and thiazole rings, in favor of the benzene ring, is seen for **BzAThMeP**. Also, some interactions of the P═O unit with the silver electrode surface are evident, and the strength of these interactions changes in the direction: **ImMeP** > **BAThMeP** > **(PyMe)$_2$P** > **(ImMe)$_2$P** ≥ **BzThMeP**. The coordination of the PC(O/N)C fragment to this surface is also very important in the case of **(ImMe)$_2$P**, **BAThMeP**, and **BzThMeP**, whereas this group assists in this coordination for **(PyMe)$_2$P**.

The observed SERS signals for all biomolecules investigated here correlate well with the contribution of the structural components to the ability of these biomolecules to interact with their receptors. As we discussed before, the arrangement of the aromatic ring on the silver electrode surface of these biomolecules varies from largely vertical for **ImMeP** and **BzAThMeP** to inclined for **(PyMe)$_2$P** and **BAThMeP** to almost horizontal for **(ImMe)$_2$P**. This is consistent with the biological activity studies for these biomolecules that show that the inhibitory activity toward chymotripsin from bovine pancrease ranges from 12 to 25% of inhibition (inhibitor concentration 23 μM, chymotripsin concentration 1.29 μM) in the following order of activity: **ImMeP** > **BzThMeP** > **(PyMe)$_2$P** > **BAThMeP** > **(ImMe)$_2$P**.[15] This fact together with the observed changes in the orientation of the O═PC(O/N)C fragment reflect a tendency for the aromatic ring and O═PC(O/N)C moiety of these peptides to approach the roughened silver electrode in a different manner, due to slightly different structuring.

Thus, the results presented here demonstrate the feasibility of using SERS spectroscopy to probe biomolecule−metal interactions that mimic the mechanism of a substrate binding to its receptor.

Acknowledgment. This work was supported by the Polish State Department for Scientific Research (Grant No. N N204 159136 to E.P.).

References and Notes

(1) Savigniac, P.; Iorga, B. *Modern Phosphonate Chemistry*; CRC Press LLC, 2003.
(2) Murphy, P. J. *Organophosphorus Reagents*; Oxford University Press, 2004.
(3) Kukhar, V. P.; Hudson, H. R. *Aminophosphnic and Aminophosphnic Acids*; John Wiley & Sons: Chichester, 2000.
(4) Ordonez, M.; Rojas-Cabrera, H.; Cativiela, C. *Tetrahedron* **2009**, *65*, 17.
(5) Kolodiazhnyi, O. I. *Tetrahedron: Asymmetry* **2005**, *16*, 3295.
(6) Hirschmann, R.; Smith, A. B., III; Taylor, C. M.; Benkovic, P. A.; Taylor, S. D.; Yager, K. M.; Sprengler, P. A.; Benkovic, S. J. *Science* **1994**, *265*, 234.
(7) Bubenik, M.; Rej, R.; Nguyen-Ba, N.; Attardo, G.; Oullet, F.; Chan, L. *Bioorg. Med. Chem. Lett.* **2002**, *12*, 1865.
(8) Grembecka, J.; Mucha, A.; Cierpicki, T.; Kafarski, P. *J. Med. Chem.* **2003**, *46*, 2641.
(9) Snoeck, R.; Holy, A.; Dewolf-Peeters, C.; Van Den Oord, J.; De Clercq, E.; Andrei, G. *Antimicrob. Agents Chemother.* **2002**, *46*, 3356.
(10) Huang, J.; Chen, R. *Heteroat. Chem.* **2000**, *11*, 480.
(11) Frechette, R. F.; Ackerman, C.; Beers, S.; Look, R.; Moore, J. *Bioorg. Med. Chem. Lett.* **1997**, *7*, 2169.
(12) Lavielle, G.; Hautefaye, P.; Schaeffer, C.; Boutin, J. A.; Cudennec, C. A.; Pierre, A. *J. Med. Chem.* **1991**, *34*, 1998.
(13) Ganzhorn, A. J.; Hoflack, J.; Pelton, P. D.; Strasser, F.; Chanal, M.-C.; Piettre, S. R. *Bioorg. Med. Chem.* **1998**, *6*, 1865.
(14) Bal, W.; Bertini, I.; Kozłowski, H.; Monnani, R.; Scozzafava, A.; Siatecki, Z. *J. Inorg. Biochem.* **1990**, *40*, 227.

(15) Olszewski, T. Unpublished results, part of PhD Thesis, Wroclaw University of Technology, Poland, 2006.
(16) Oleksyszyn, J.; Powers, J. C. *Biochemistry* **1991**, *30*, 485.
(17) Oleksyszyn, J.; Boduszek, B.; Kam, C.-M.; Powers, J. C. *J. Med. Chem.* **1994**, *37*, 226.
(18) Olszewski, T. K.; Gałęzowska, J.; Boduszek, B.; Kozłowski, H. *Eur. J. Org. Chem.* **2007**, 3539.
(19) Olszewski, T. K.; Boduszek, B.; Sobek, S.; Kozłowski, H. *Tetrahedron* **2006**, *62*, 2183.
(20) Andrzejak, M.; Podstawka, E.; Boduszek, B.; Olszewski, T. K.; Proniewicz, L. M. *J. Phys. Chem. B*, To be submitted.
(21) Podstawka, E. *Biopolymers* **2008**, *89*, 506.
(22) Podstawka, E *J. Raman Spectrosc.* **2008**, *39*, 1290.
(23) Podstawka, E.; Kafarski, P.; Proniewicz, L. M. *J. Phys. Chem. A* **2008**, *112*, 11744.
(24) Podstawka, E.; Proniewicz, L. M. *J. Phys. Chem. B* **2009**, *113*, 4978.
(25) Podstawka, E.; Kudelski, A.; Drąg, M.; Oleksyszyn, J.; Proniewicz, L. M. *J. Raman Spectrosc.*, in press.
(26) Podstawka, E.; Kudelski, A.; Proniewicz, L. M. *Surf. Sci.* **2007**, *601*, 4971.
(27) Podstawka, E.; Kudelski, A.; Kafarski, P.; Proniewicz, L. M. *Surf. Sci.* **2007**, *601*, 4586.
(28) Markham, L. M.; Mayne, L. C.; Hudson, B. S.; Zgierski, M. Z. *J. Phys. Chem.* **1993**, *97*, 10319.
(29) Cao, P.; Gu, R.; Tian, Z. *J. Phys. Chem. B* **2003**, *107*, 769.
(30) Carter, D. A.; Pemberton, J. E. *Langmuir* **1992**, *8*, 1218.
(31) Bukowska, J.; Kudelski, A.; Jackowska, K. *J. Electroanal. Chem.* **1991**, *309*, 251.
(32) Leygraf, C.; Thierry, D. *J. Electrochem. Soc.* **1986**, *133*, 2236.
(33) Xue, G.; Dai, Q.; Jiang, S. *J. Am. Chem. Soc.* **1988**, *110*, 2393.
(34) Siiman, O; Rivehi, R.; Patel, R. *Inorg. Chem.* **1988**, *27*, 3940.
(35) Davis, K. L.; McGlashen, M. L.; Morris, M. D. *Langmuir* **1992**, *8*, 1654.
(36) Martusevicius, S.; Niaura, G.; Talaikyte, Z.; Razumas, V. *Vib. Spectrosc.* **1996**, *10*, 271.
(37) Picquart, M.; Lacrampe, G.; Jaffrain, M. *Spectroscopy of Biological Molecules*; MIX, A. J. P., Bernard, L., Manfait, M., Eds.; Wiley: Chicheater, 1985; p 190.
(38) Nabiev, I. R.; Savchenko, V. A; Efremov, E. S. *J. Raman Spectrosc.* **1983**, *14*, 375.
(39) Hegelund, F.; Wugt Larsen, R.; Palmer, M. H. *J. Mol. Struct.* **2007**, *244*, 63.
(40) Palmer, M. H. *J. Mol. Struct.* **2007**, *834*−*836*, 113.
(41) El-Azhary, A. A.; Ghoneim, A. A.; El-Shakare, M. E. *J. Chem. Res* **1995**, *9*, 354, Miniprint, 2123.
(42) Zuo, Ch.; Jagodziński, P. W. *J. Phys. Chem. B* **2005**, *109*, 1788.
(43) Vivoni, A.; Birke, R. L.; Foucault, R.; Lombardi, J. R. *J. Phys. Chem. B* **2003**, *107*, 5547.
(44) Ingram, J. C.; Pemberton, J. E. *Langmuir* **1992**, *8*, 2034.
(45) Johnson, C. K.; Soper, S. A. *J. Phys. Chem.* **1989**, *93*, 7281.
(46) Arenas, J. F.; Tocon, I. L.; Otero, J. C.; Marcos, J. I. *J. Phys. Chem.* **1996**, *100*, 9254.
(47) Creighton, J. A. *Surf. Sci.* **1985**, *158*, 211.
(48) Pemberton, J. E.; Carter, D. A. *Langmuir* **1992**, *8*, 1218.
(49) Campion, A.; Kambhamapati, P. *Chem. Soc. Rev.* **1998**, *27*, 241.
(50) Creighton, J. A. *Spectroscopy of surfaces*; Clark, R. J., Hester, R. E., Eds.; Wiley: New York, 1998; chapter 2.
(51) Cao, P.; Gu, R.; Tian, Z. *J. Phys. Chem. B* **2003**, *107*, 769.
(52) Lombardi, J. R.; Birke, R. L. *J. Phys. Chem. C* **2008**, *112*, 5605.
(53) Bukowska, J.; Fackowska, K.; Jaszczynski, K. *J. Electroanal. Chem.* **1989**, *260*, 373.
(54) Muniz-Miranda, M.; Neto, N.; Sabrana, G. *J. Phys. Chem.* **1988**, *92*, 954.
(55) Castro, J. L.; López Ramírez, M. L.; Lopez Tocón, I.; Otero, J. C. *J. Colloid Interface Sci.* **2003**, *263*, 357.
(56) Arenas, J. F.; Soto, J.; López-Tocón, I.; Fernández, D. J.; Otero, J. C.; Marcos, J. I. *J. Chem. Phys.* **2002**, *116*, 7207.

JP902328J